Measurement of the Magnetic Moment of the Λ^0 Hyperon*

R. L. Cool, E. W. Jenkins, and T. F. Kycia
Brookhaven National Laboratory, Upton, New York

D. A. Hill
Laboratory for Nuclear Science, Massachusetts Institute of Technology, Cambridge, Massachusetts

L. Marshall
New York University, New York, New York

AND

R. A. Schluter
Argonne National Laboratory, Argonne, Illinois, and Northewestern University, Evanston, Illinois

(Received May 3, 1962)

A measurement of the magnetic moment of the Λ^0 hyperon carried out at the Brookhaven Cosmotron gives the value $\mu_{\Lambda^0} = -1.5\pm0.5$ Bohr nucleon magnetons. Polarized Λ^0 hyperons were produced by 1.02 ± 0.03 BeV/c π^+ mesons incident on a Be target in the reaction $\pi^+ + n \rightarrow \Lambda^0 + K^+$. After passing through a strong magnetic field, the Λ^0 were observed to decay in a parallel plate spark chamber which was triggered by an electronic counter logic. The asymmetry of the π^- from the decay $\Lambda^0 \rightarrow \pi^- + p$ provided the method for determining the axis of polarization. The magnetic field and flight path were such that a magnetic moment of one Bohr nucleon magneton would precess $16.5°$ in a plane perpendicular to the Λ^0 trajectory. Measurement of the angle of rotation of the decay pattern with field on, off, and reversed gave the magnitude of the moment; the sense of rotation yielded the sign.

INTRODUCTION

DURING the years following the discovery of hyperons in 1947,[1] a considerable fraction of the effort in high-energy particle physics has been directed toward the measurement of their intrinsic properties. In most cases the mass, charge, spin, lifetime, and decay modes are already reasonably well established. The possibility of measuring their magnetic moments was also visualized almost as soon as they were available in appreciable numbers from laboratory accelerators.[2,3] We report here the first measurement of the magnetic moment of one of them, the Λ^0 hyperon.

Besides the importance of the magnetic moment in characterizing the interaction of a particle with an external electromagnetic field, the present state of the theory of strong interactions also gives hope that a knowledge of this constant will provide an insight into the internal structure of the particle. Indeed, in the present view, it should be possible to calculate the magnetic moment from a knowledge of the symmetries of the baryon and meson fields and their coupling constants. While this ultimate goal has not yet been realized even for the nucleons, experimental values for the hyperon moments should provide valuable check points for the testing of new ideas in the theory of the strong interactions.

The fact that parity is not conserved in the decay $\Lambda^0 \rightarrow p + \pi^-$ leads to the well-known asymmetry in the angular distribution of the pion with respect to the direction of the spin polarization.[4] Since the effective magnetic moment and the spin must be parallel or antiparallel, the angular distribution of the decay can be utilized to measure the orientation of the magnetic moment for a sample of polarized Λ^0 hyperons.

If polarized Λ^0 hyperons are placed in a strong magnetic field which is perpendicular to the polarization axis, they will precess about the magnetic field with the classical Larmor frequency. A measurement of the rotation of the decay pattern gives a quantitative measure of the magnitude and sign of the moment.

EXPERIMENTAL PROCEDURE

The general method outlined briefly above requires a source of polarized Λ^0 hyperons. The reaction $\pi^- + p \rightarrow \Lambda^0 + K^0$ is known[4] to produce highly polarized Λ^0 at momenta near 1.0 BeV/c; a large polarization has also been observed by electronic techniques for the charge symmetric reaction[5] $\pi^+ + n \rightarrow \Lambda^0 + K^+$ when the neutron is bound in D_2. In the choice between these known reactions, two factors played a decisive role. First, the requirement that the uncertainty in the point of origin of the Λ^0 be small compared to the average flight path dictated a small target. Second, the yield of Λ^0 was clearly the limiting factor on accuracy. When coupled with the first, a target of high density was strongly indicated. Thus, since a target of bound nucleons appeared necessary, the ease of detection of the K^+ compared to the K^0 led to the choice of $\pi^+ + n \rightarrow \Lambda^0 + K^+$ and

---

[1] G. D. Rochester and C. C. Butler, Nature **160**, 855 (1947).
[2] M. Goldhaber, Phys. Rev. **101**, 1828 (1956).
[3] T. D. Lee and C. N. Yang, Phys. Rev. **108**, 1645 (1957).

[4] F. S. Crawford, M. Cresti, M. L. Good, K. Gottstein, E. M. Lyman, F. T. Solomitz, M. L. Stevenson, and H. Ticho, Phys. Rev. **108**, 1102 (1957).
[5] R. L. Cool, B. Cork, J. W. Cronin, and W. A. Wenzel, Phys. Rev. **114**, 912 (1959); B. Cork, L. Kerth, W. A. Wenzel, J. W. Cronin, and R. L. Cool, *ibid.* **120**, 1000 (1960).
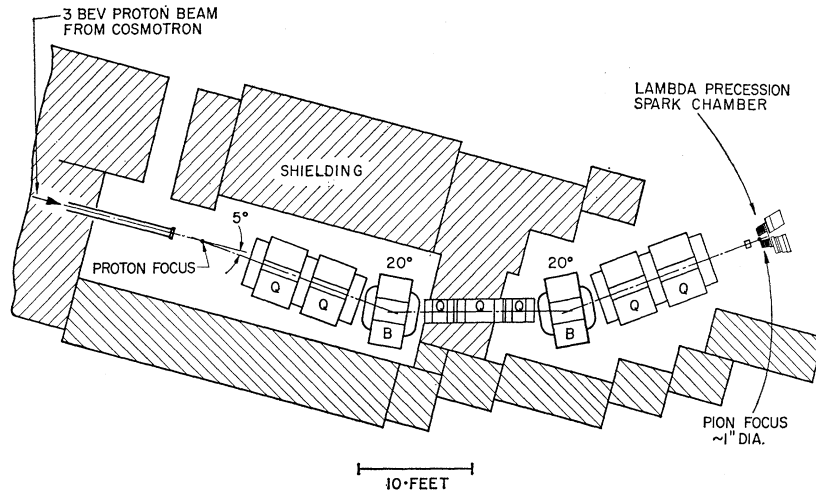
FIG. 1. Schematic plan view of the 1.02-BeV/c π^+ beam at the Brookhaven Cosmotron showing the external proton beam, pion production target, and quadrupole magnet lens system.

the use of Be as a target material. The beam momentum was chosen as 1020 MeV/c corresponding to the peak of the Λ^0 production cross section. This momentum is very near the Σ^0 production threshold so that contamination from this reaction was negligible.

The choice of a target of bound nucleons brings with it several problems in the design of the experiment. (1) The Fermi momentum of the nucleons within the nucleus "smears out" the kinematic relationships between angles and momenta for the process. (2) The interaction of the Λ^0 with nucleons within the producing nucleus might appreciably depolarize the source. Since D_2 did not appear to give appreciable depolarization,[5] Be was selected as the lightest nucleus consistent with our target density requirements.
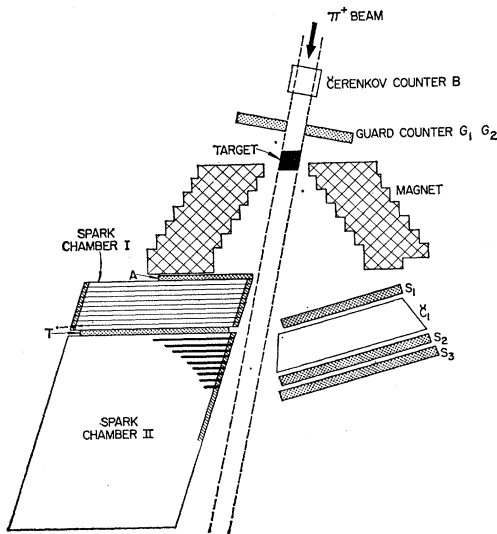

FIG. 2. Schematic diagram of equipment for the detection of the precession of the Λ^0 magnetic moment, showing Λ^0 production target, precession magnet, particle detection counters, and the spark chamber in which the Λ^0 decays were photographed.

The pion beam was designed[6] to achieve the maximum intensity within an aperture of 1.25 in.$\times$1.25 in. at the target. The magnetic lens system limited the band width of transmitted pion momenta to less than that which could otherwise have been tolerated by the experimental arrangement. Figure 1 shows a schematic view of the magnet arrangement. To a first approximation the system is symmetrical with the first doublet focusing the proton target at the center of the central triplet lens. The final quadrupole doublet refocuses this image at the Be target of the apparatus. The central triplet acts essentially as a field lens. The bending magnets select the momentum, and the deflections are so related that the images of different momenta are recombined at the target. Detailed trajectories were calculated using an LGP 30 computer which showed that the bandwidth of momentum was limited within the acceptable aperture to ±30 MeV/c. The final beam of 1020 ± 30 MeV/c had a flux of 2×10^5 π^+ and 6×10^5 protons per 10^{11} circulating protons; the average circulating beam was 4×10^{10} per pulse. Magnet currents were adjusted to very nearly their final values using a photographic beam profile detector,[7] the last adjustments being deduced from particle counter traverses across the beam.[8]

Figure 2 shows a schematic view of the apparatus. The Čerenkov counter (B), filled with liquid fluorochemical FC75, was sensitive to beam pions, but not to protons of the same momentum. Guard counters (G_1G_2) in anticoincidence required that no charged particle of the beam which hit the magnet walls could trigger the spark chamber. An anticoincidence counter (A) at the entrance to the spark chamber ensured that the Λ^0 had not decayed before it entered the chamber. The scintil-

lation counter (T), placed between the first and second spark chambers, required that the Λ^0 had decayed into charged particles before reaching it. In order to minimize conversion of photons and neutrons, the first spark chamber was made of thin plates, namely, 8-mil stainless steel foil. The spark chambers following the coincidence counter (T) were made with 1/8 in. brass plates in order to stop the decay proton and sometimes the decay pion within the chamber.

After striking the target, the pion beam passed through the magnet and exited between the spark chamber on the one side and the K-meson telescope on the other. The K-meson telescope consisted of three plastic scintillation counters $(S_1S_2S_3)$ and of one Čerenkov counter (C_1) filled with water and connected in anticoincidence. The latter was sensitive only to particles having $\beta > 0.75$. The kinematics of the production reaction are such that the desired K mesons have $\beta < 0.75$. Thus, the telescope selects preferentially the desired reaction, but does not require it exclusively. A schematic diagram of the electronic logic is shown in Fig. 3. The occurrence of a signal characterized by the multiple coincidence $B\bar{G}_1\bar{G}_2\bar{A}\,T\bar{C}S_1S_2S_3$ triggered the onset of a high-voltage pulse to the plates of the spark chamber. Subsequent electrical discharges along the tracks of charged particles in the chamber were photographed.

The target was a rectangular parallelopiped of beryllium 1 1/4 in.$\times$1 1/4 in.$\times$1 1/2 in., the longest dimension lying parallel to the beam. The distance from the center of the target to the first plate of the spark chamber was 6.47 in. along the direction of the beam, but was 7.18 in. along the average line of flight of the Λ^0. The spark chamber accepted Λ^0 hyperons produced between 55 and 168° barycentric angle.

The magnet was a flared solenoid, constructed of seven double pancakes, wound with internally water cooled copper conductor 5/8-in. o.d. and 3/8-in. i.d. The magnet was 2 in.$\times$2 in. i.d. in cross section at the entrance, 6 in. deep, and 3 in.$\times$8 in. i.d. cross section at the exit. Each pancake was wound with Fiberglas tape
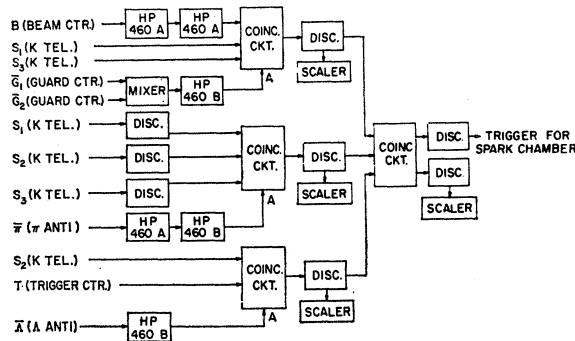

FIG. 3. Schematic diagram of electronic logic for the particle detectors which trigger the onset of the high voltage pulse to spark chamber.
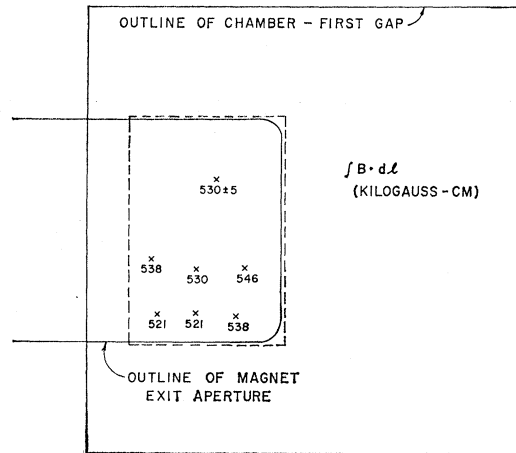

FIG. 4. Schematic diagram indicating values of integral of magnetic field measured along various orientations of the flight path of the Λ^0.

and impregnated with epoxy resin. The pancakes were connected in series to a 1.2 MW generator and pulsed to about 5500 A with 0.3-sec rise time, 0.7-sec pulse width, in such a way as to reach maximum magnetic field at a time coincident with the beam pulse of the Cosmotron.

The variation of magnetic field during the 30-msec beam pulse of the Cosmotron was about 3% throughout the duration of the experiment. Its variation was recorded on the spark-chamber film by photographing the magnet current signal displayed on an oscilloscope. The integral of magnetic field along the various possible paths which a Λ^0 might take between the target and the spark chamber was evaluated by measuring the current induced by a magnetic field pulse in a solenoidal coil extending along the path. The integral was found to have essentially a constant value for the various allowed paths; measured values of the field integral are indicated in Fig. 4. Except in the fringing field of the magnet near the decay point, the field was everywhere parallel to the line of flight. In principle, a correction for the transverse component, transformed to the rest system of the Λ^0, should be made. However, no correction has been made to the data for this effect since it would have been much smaller than the statistical errors. The direction of the magnetic field was reversed approximately every 12 h during the course of this experiment. In addition, about 15% of the data was taken in the same geometry with the magnetic field off.

The heavy spark chambers were made of plates of 1/8 in. brass spaced 1/4 in. apart, and the light chamber was made of 8-mil stainless steel foil spaced by 1/4 in. gaps. Stainless steel was used instead of brass in the first spark chamber to reduce the electromagnetic reaction force caused by pulsing the precession magnet. All chambers contained flowing Neon gas at slightly more than 1 atm. The fiducial marks were made on a

Lucite light pipe running along the edge of the spark chamber. They were illuminated by flashlight bulbs at either end.

The direction of the incident pion momentum p_{in} and the Λ^0 momentum, p_Λ, determine the production plane. The Λ^0 hyperon spin is polarized along the direction $(p_{in}\times p_\Lambda)$.[9] Nonconservation of parity in the charged mode of hyperon decay produces an asymmetry of the decay pions with respect to the hyperon spin direction. The form of the asymmetry is $(1+A\cos\theta)$ where θ is the angle in the c.m. between the direction of the decay pion momentum p_{out} and the hyperon spin.

Data were taken for the three situations, magnetic field aligned either parallel (P) or antiparallel (A) to p_Λ, or turned off (N). The events selected by the particle counter logic were photographed from two nearly orthogonal directions each of which was approximately normal to the direction of motion of the Λ^0. The films were measured with Hydel digitized machines; the space angles and ranges and corresponding momenta were evaluated with the AEC NYU IBM 7090 and the Argonne IBM 704 computers. The direction cosines for the line from the center of the target to the apex of the Λ^0 (the direction cosines for the vector p_Λ) were computed. Two conditions were imposed: (1) that the $\varphi_{1\Lambda}+\varphi_{2\Lambda}=\varphi_{12}$, where $\varphi_{j\Lambda}$ is the angle between prong j and p_Λ, φ_{12} being the angle between the two prongs, and (2) that the two prongs should be coplanar with p_Λ. In the computation the point of origin of the Λ^0 was varied over 27 positions corresponding to the maximum dimensions of the target and the angles were computed for which the above conditions were best approximated. Events for which these tests failed by significant amounts were rejected.

Each event was inspected for compatibility with Λ^0 decay kinematics, for distinguishability of the prongs as
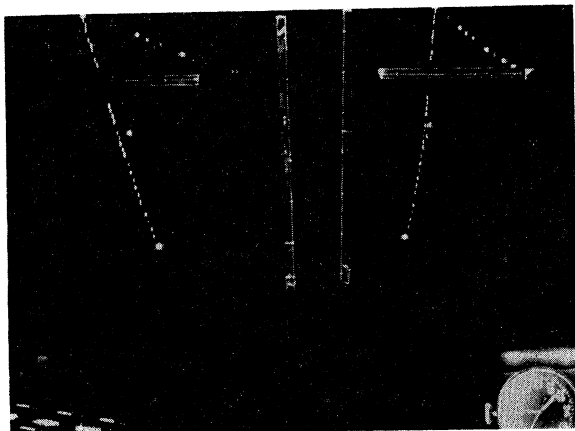

FIG. 5. An example of a Λ^0 event in a spark chamber photograph.

[9] R. W. Birge and W. B. Fowler, Phys. Rev. Letters **5**, 254 (1960); E. F. Beall, B. Cork, D. Keefe, P. G. Murphy, and W. A. Wenzel, *ibid.* **7**, 285 (1961); J. W. Cronin (private communication).
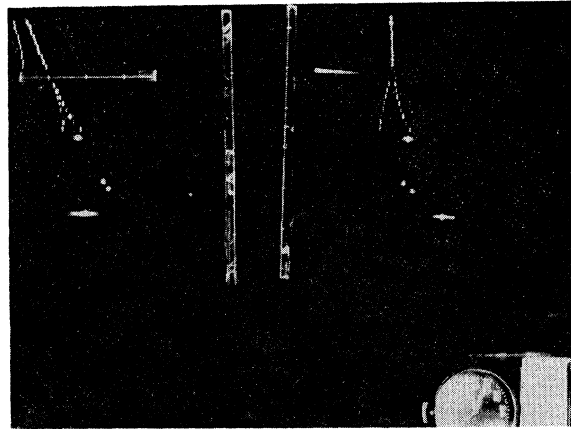

FIG. 6. Spark-chamber photograph of an electron pair from a photon converted in the plates of the thin foil spark chamber.

proton or pion, and for additional features such as consistency of scattering and delta-ray production, and relative ionization with identification of the prongs. To be included in the final analysis an event had to be accepted by at least two independent inspections. An example of such an event is shown in the photograph in Fig. 5.

The main background which might have been confused with Λ^0 decays consisted of electron pairs from gamma rays converted in the thin plates of the first spark chamber (see Fig. 6). To prevent this confusion, all events having opening angles of 10° or less were rejected. About one-third of otherwise acceptable events did not permit identification of prongs and so were rejected because, for example, their ranges and their respective angles to the Λ^0 momentum direction were so nearly equal as to be ambiguous. This was also the situation sometimes when neither prong stopped in the spark chamber so that only minimal ranges could be evaluated.

RESULTS

The lifetime of the Λ^0 evaluated from the distribution of Λ^0-decay vertices as a function of distance from the target was $(2.25\pm0.35)\times10^{-10}$ sec. This value is in agreement with the accepted value $(2.51\pm0.09)\times10^{-10}$ sec.[10] The composite distribution including all accepted events, P, N, and A, is shown in Fig. 7. This result demonstrates that the accepted sample of events consists of Λ^0 hyperons with a contamination of spurious events small enough to be neglected for our purpose.

The composite momentum distribution of all accepted events ($P+A+N$ distributions) is shown in Fig. 8. It is in agreement with that expected for 1.02-BeV/c pions incident on bound neutrons, when one assumes the usual Fermi momentum distribution.

[10] A compilation is given by W. H. Barkas and A. H. Rosenfeld, *Proceedings of the 1960 Annual International Conference on High-Energy Physics at Rochester* (Interscience Publishers, Inc., New York, 1960), p. 878.

About 800 events were accepted as Λ° hyperons with identifiable prongs. Their positions of decay were found to be homogeneously distributed when projected on a plane normal to the beam. This fact was independently true for all three distributions (P,A,N). The direction cosines of $\mathbf{p}_\Lambda$ for the no-field (N) events were found to be equally distributed above and below the median plane of the apparatus. These tests show that the axis perpendicular to the median plane defined by the K telescope and spark chamber corresponds to the axis $\mathbf{p}_{in}\times\mathbf{p}_\Lambda$ for the no-field situation and that switching on the magnetic field introduces in the flight path of the K^+ mesons no detectable asymmetry with respect to the two field directions.

In the initial scanning, measuring and kinematic checking process, all identified Λ° hyperons were included, independent of the position of the vertex within the spark chamber. It was expected that for those vertices close to the chamber wall, there would appear a
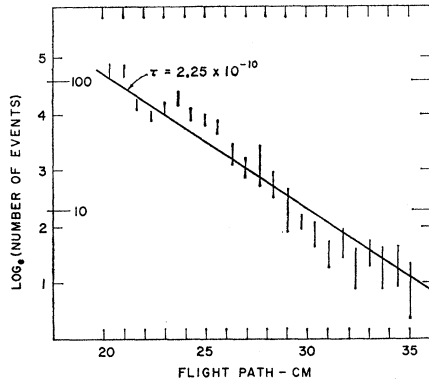

FIG. 7. Composite distribution of Λ°-decay events vs distance from target, for all events of P, A, and N distributions combined. The solid line corresponds to a Λ° lifetime of $(2.25\pm0.35)\times10^{-10}$ sec.

bias against the identification of those hyperons in which the decay pion was directed toward the near wall. In this apparatus, only the spark-chamber wall nearest the beam was sufficiently close to the origin of the events to introduce such a bias.

To evaluate and eliminate such a possible bias, the following procedure was adopted. For the no-field events, there should be equal numbers of events in which the decay pion is in the hemisphere toward the wall as in that away from the wall, if the sample is unbiased. Similarly, a second sample consisting of equal numbers of events with field parallel and antiparallel should exhibit equal numbers in the two hemispheres independent of the magnetic moment, if there is no selection bias. For both samples, the ratio of the numbers of events in the two hemispheres was computed as a function of the distance of the vertex from the wall. For the events within 0.5 in. of the wall the bias is severe; it is moderate for those between 0.5 and 1.0 in.; but, within error, is
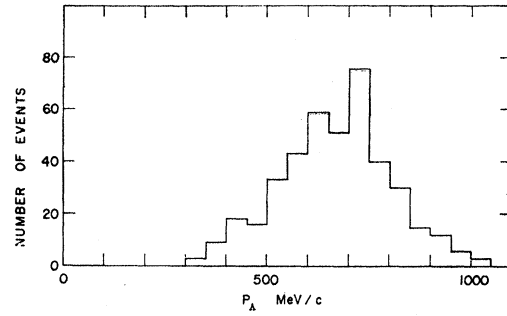

FIG. 8. The composite momentum distribution of all Λ° events, $P+A+N$.

absent for those more than 1.0 in. from the wall. As a consequence, only those events whose vertex lies further than 1.0 in. from the wall were accepted for the subsequent magnetic moment analysis. This choice reduced the number of acceptable events by a factor of two.

It is most convenient to write the angular distribution of the decay pion from the Λ° decay in terms of an angle η which is the angle between the direction $\mathbf{p}_{in}\times\mathbf{p}_{\Lambda^0}$ and the projection of the pion momentum $\mathbf{p}_{out}$ on the plane perpendicular to the Λ° momentum $\mathbf{p}_{\Lambda^0}$ (see Fig. 9). The angular distribution is given by

$$N(\eta)d\eta = (N_0/2\pi)[1+K\cos\eta]d\eta, \qquad (1)$$

where N_0 is the total number of events. The distribution (1) is the same for both the c.m. and laboratory reference frames. Thus, all angles can be directly measured in the laboratory system and no c.m. transformations are required.

The presence of the magnetic field H acting on a magnetic moment μ_0 normal to H causes it to precess about H with frequency $\omega=\mu_0 H/Ih$. The angle of rotation ϵ, after time t is ωt, which can be written

$$\epsilon = 2.74\times10^5 gHt/\gamma \quad (\text{deg}), \qquad (2)$$

where the gyromagnetic ratio $g=\mu_0/I$, (μ_0 is in Bohr nucleon magnetons, the time spent in the field $t=d/\beta c$ in seconds, H is in Gauss, and I is the spin). The factor of $\gamma=(1-v^2/c^2)^{-1/2}$ in the denominator corrects for the relativistic increase in mass of the moving hyperon. If spin and magnetic moment are parallel, $g>0$; if antiparallel, $g<0$. The sense of the rotation depends only on the algebraic sign of g and the direction of H. It is
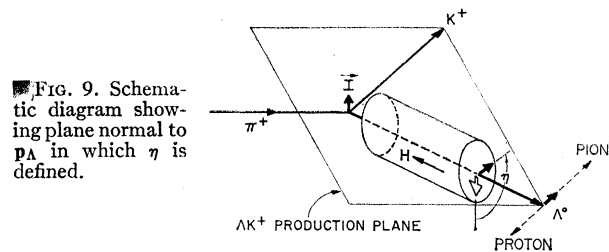

FIG. 9. Schematic diagram showing plane normal to $\mathbf{p}_\Lambda$ in which η is defined.

implied by the equation $\Delta \mathbf{I} = g\mathbf{I}\times\mathbf{H}$. Thus, in the presence of a magnetic field the whole angular distribution (1) is rotated by angle ϵ:

$$N(\eta)d\eta = (N_0/2\pi)[1+K\cos(\eta-\epsilon)]d\eta. \qquad (3)$$

For the purpose of evaluating the angular rotations ϵ, and their errors, it is advantageous to use integrals of the distribution (3). We define

$$N_L = \frac{N_0}{2\pi}\int_\delta^{\delta+\pi}[1+K\cos(\eta-\epsilon)]d\eta$$

$$= \frac{N_0}{2\pi}[\pi-2K\sin(\delta-\epsilon)], \qquad (4a)$$

and similarly

$$N_R = \frac{N_0}{2\pi}\int_{\delta+\pi}^{\delta+2\pi}[1+K\cos(\eta-\epsilon)]d\eta$$

$$= \frac{N_0}{2\pi}[\pi+2K\sin(\delta-\epsilon)], \qquad (4b)$$

where the angle δ is measured in the plane perpendicular to the line of flight of the Λ^0 and is equal to zero for the
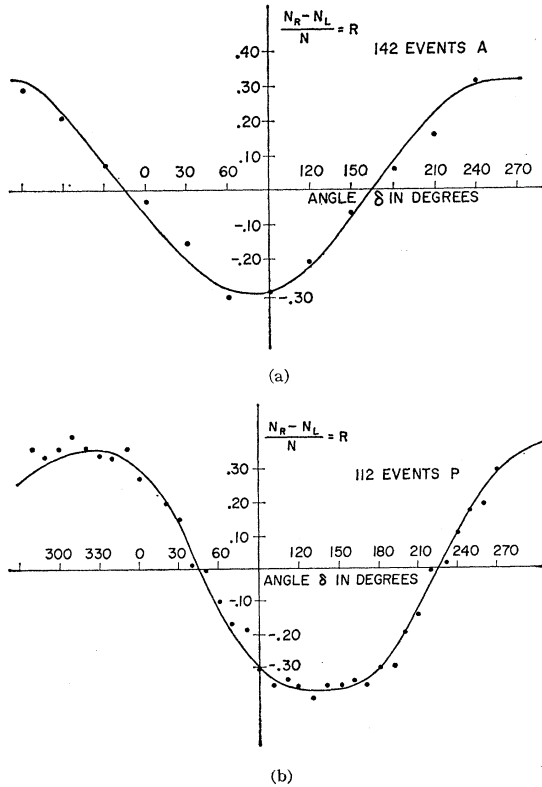

(a)

(b)

FIG. 10. The ratio R (Eq. 5) plotted vs the parametric angle δ for the A and P distributions of Λ^0 events. The value of δ at which $R=0$ corresponds to the most probable angle of rotation of the Λ^0 magnetic moment.

TABLE I. Best values of the angle ϵ and the amplitudes obtained from the experimental R distributions.

Distribution	No. of events	$2K/\pi$	ϵ in degrees
A	142	0.32±0.13	$-15°\pm15°$
P	112	0.35±0.15	$+45°\pm15°$
N	54	0.34±0.21	$-4°\pm23°$

direction $\mathbf{p}_{\pi\,\text{in}}\times\mathbf{p}_{\Lambda^0}$. Then the ratio

$$R = (N_R-N_L)/N_0 = (2K/\pi)\sin(\delta-\epsilon). \qquad (5)$$

From (5), it is clear that the R distributions should pass through zero for $\epsilon=\delta$; with field parallel (P) and antiparallel (A), the values of ϵ should be equal, within the error, but opposite in sign. For no field, $\epsilon=\delta$ should be zero within errors. The magnitude of the amplitudes for the three cases should be the same and equal to $2K/\pi$.

The standard deviation errors in the value of ϵ for each field configuration are given by

$$\Delta\epsilon = \pi/2K\sqrt{N_0}, \qquad (6)$$

and for the amplitude by

$$\Delta K = \pi/2\sqrt{N_0}. \qquad (7)$$

The experimental R distributions are given in Figs. 10 and 11. The solid line curves are sine functions which clearly fit the data well in all cases. This fact shows that there are no appreciable biases in the events selected within the fiducial volume. The best values of the angle ϵ and the amplitudes obtained from these distributions are given in Table I. From Table I, the mean value of $|\epsilon|$ is then $30\pm11°$; and for the amplitude K is 0.52 ±0.14. It is important to note that the sign of ϵ in Table I is reversed for the A and P distributions and that the absolute values of each one are, within error, consistent with the mean value given above. We conclude that the reversal of sign is due to the magnetic field, and is unlikely to be due to statistical fluctuations, the difference being $60\pm21°$.

For obtaining the optimum values of the parameters ϵ and K from the three sets of data P, A, and N we have used the maximum likelihood procedure. The likelihood functions are given by

$$\varphi_P = \prod_{j=1}^{N_P}[1+K\cos(\eta_j-\epsilon)], \qquad (8a)$$

$$\varphi_A = \prod_{j=1}^{N_A}[1+K\cos(\eta_j+\epsilon)], \qquad (8b)$$

$$\varphi_N = \prod_{j=1}^{N_N}[1+K\cos(\eta_j)]. \qquad (8c)$$

We assume that the values of ϵ and K found from the

data have a Gaussian relationship to the true values ϵ_0 and K_0.

The optimum value of ϵ is then obtained from the condition that

$$\partial \ln(\varphi_A \varphi_P \varphi_N)/\partial \epsilon = 0, \qquad (9)$$

which gives

$$\sum_{j=1}^{N_A} \frac{d_j}{P_j} \frac{\sin(\eta_j + \epsilon)}{K^{-1} + \cos(\eta_j + \epsilon)}$$

$$- \sum_{j=1}^{N_P} \frac{d_j}{P_j} \frac{\sin(\eta_j - \epsilon)}{K^{-1} + \cos(\eta_j - \epsilon)} = 0. \quad (10)$$

This equation we call the F equation, briefly,

$$F = F_A - F_P = 0. \qquad (11)$$

The factor d_j/P_j occurs from the derivative of ϵ which depends, for each event, on the distance between target and vertex, d_j, and the momentum P_j.
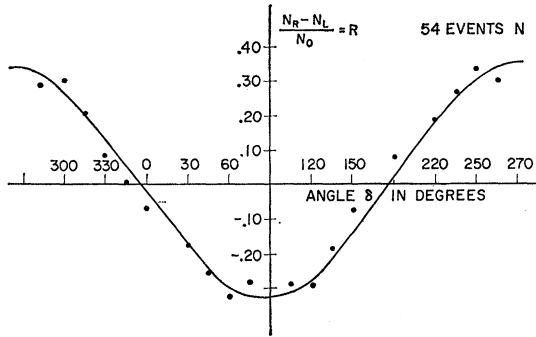
FIG. 11. The ratio R [Eq. (5)] plotted vs the parametric angle δ for the no-field distribution (N) of Λ^0 events.

Similarly, the optimum value of K is obtained from the condition that

$$\partial \ln(\varphi_A \varphi_P \varphi_N)/\partial K = 0, \qquad (12)$$

which gives

$$\sum_{j=1}^{N_A} \frac{\cos(\eta_j + \epsilon)}{K^{-1} + \cos(\eta_j + \epsilon)} + \sum_{j=1}^{N_P} \frac{\cos(\eta_j - \epsilon)}{K^{-1} + \cos(\eta_j - \epsilon)}$$

$$+ \sum_{j=1}^{N_N} \frac{\cos\eta_j}{K^{-1} + \cos\eta_j} = 0. \quad (13)$$

This equation we call the G equation; briefly,

$$G = G_A + G_P + G_N = 0. \qquad (14)$$

The two simultaneous equations (11) and (14) were solved numerically using an IBM computer. The five functions F_A, F_P, G_A, G_P, and G_N were evaluated for seven values of K from 0.10 to 0.70 and at intervals of 5° for values of ϵ ranging from 0° to 360°.

By superposition of the two maximum-likelihood contour plots, Figs. 12 and 13, one obtains as the
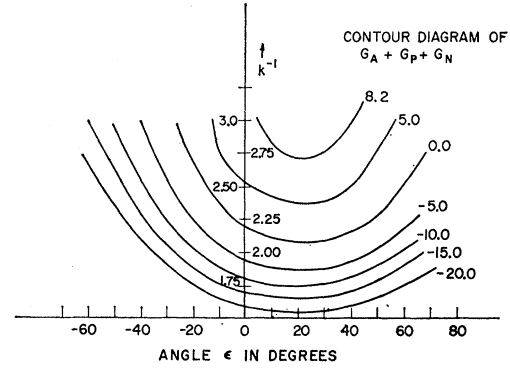

FIG. 12. Contour diagram of the G function for the distribution of data A, P, and N plotted against the parameters K^{-1} and ϵ.

simultaneous solution of Eqs. (11) and (14) the values $\epsilon_0 = 25$ deg and $K_0 = 0.46$. The standard deviation error on ϵ_0 is given by the relationship

$$\sigma = \left[\{\partial^2 \ln\Phi/\partial\epsilon^2\} \frac{p}{D} \right]^{-1/2} \text{ radians}, \qquad (15)$$

where $\Phi = \Phi_A \Phi_P \Phi_N$, $p = 680$ MeV/c, the average momentum, and where D is 9.4 in., the average flight path. From the contour diagram of the F functions one finds that $\partial \ln\Phi/\partial\epsilon$ changes by 0.10 for $\Delta\epsilon = 12°$ at $\epsilon_0 = 25°$, so that $\sigma = 0.14$ radian or 8°.

Inserting in Eq. (2) the average value of the field integral (see Fig. 4) of 540 kG-cm, and the average momentum, for which $\beta\gamma = 0.61$, $\epsilon = 8.25g$ (deg). Since the spin has been found[11] to be 1/2, $g = 2$ and $\epsilon = 16.5°$ for one Bohr nucleon magneton. The observed value of $\epsilon = 25° \pm 8°$, then gives $\mu_0 = -1.5 \pm 0.5$ Bohr nucleon magnetons. The negative sign is obtained from the
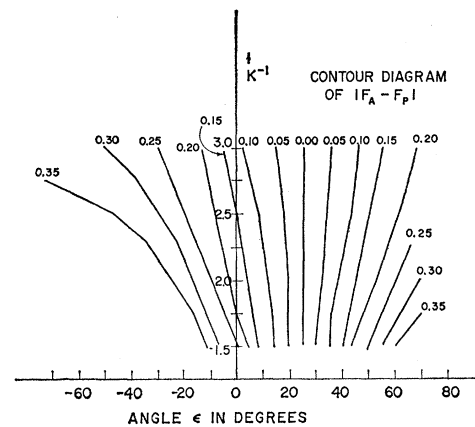

FIG. 13. Contour diagram of the F function for distributions of data A and P plotted against the rotation angle ϵ and the reciprocal of the asymmetry parameter, K^{-1}. In this notation, the rotation angle ϵ is introduced in the P distribution in the form $(\eta - \epsilon)$ whereas in the A distribution it is $(\eta + \epsilon)$. The condition $F_A = F_P$ is realized for $\epsilon = 25°$ for a wide range of values of K.

[11] T. D. Lee and C. N. Yang, Phys. Rev. 109, 1755 (1958).

observation that the rotation of the decay pattern is like that of a right-handed screw moving along the direction of the magnetic field.

The parameter K is directly related to $\alpha\bar{P}$, where α is the asymmetry parameter and $\bar{P}$ is the polarization. From a knowledge of the limits of opening angles accepted in Λ^0 decays, we have obtained the value of $\alpha\bar{P}$ for Λ^0 hyperons produced in Be within the barycentric angles 55 to 165°. We find $\alpha\bar{P}=0.55\pm0.10$.

Although attempts have been made to compute magnetic moments of hyperons,[12] and in particular predictions have been made for the magnetic moment of the Λ^0 from baryon models involving symmetries higher than charge independence,[13] there is as yet no generally accepted theory of baryons which predicts the measured value for the magnetic moment of the Λ^0. Under the assumption that mass differences of the baryons can be neglected, Coleman and Glashow predict the value $\frac{1}{2}\mu_N$, while Cabbibo and Gatto using the Sakata model find $\mu_{\Lambda^0}=\mu_N$. A simple model[14] of the Λ^0, represented as a K meson in an orbit of angular momentum $l=1$ about a nucleon, would have a magnetic moment[15] of -0.78

nuclear magneton and, in addition, would predict an even parity for the (ΛKN) system, consistent with presently accepted ideas.[16]

Note added in proof. Kernan, Novey, Warshaw, and Wattenberg reported the results of an experiment to measure the magnetic moment of the Λ^0 at the 1962 International Conference on High Energy Physics at CERN. Their experiment gave $\mu_{\Lambda^0}=0\pm0.6$ nucleon magnetons, a result which, except for statistical uncertainties, disagrees with our value reported above.

[12] For example: H. Katsumori, Prog. Theoret. Phys. (Kyoto) 18, 375 (1957); R. E. Marshak, S. Okubo, and G. Sudarshan, Phys. Rev. 106, 5999 (1957); W. G. Holladay, *ibid*. 115, 1331 (1959); K. Tanaka, *ibid*. 122, 705 (1961); N. Cabbibo and R. Gatto, Nuovo cimento 21, 871 (1961).
[13] G. Feinberg and R. E. Behrends, Phys. Rev. 115, 745 (1959); S. Coleman and S. L. Glashow, Phys. Rev. Letters 6, 423 (1961); R. E. Behrends and A. Sirlin, Phys. Rev. 121, 324 (1961).
[14] M. Goldhaber, Phys. Rev. 101, 433 (1956).
[15] L. Landovitz (private communication).

[16] M. Block, A. Engler, R. Gessaroli, J. Kopelman, M. Meer, A. Pevsner, P. Schlein, R. Strand, L. Grimellini, L. Lendenara, and L. Monari, Bull. Am. Phys. Soc. 7, 49 (1962).

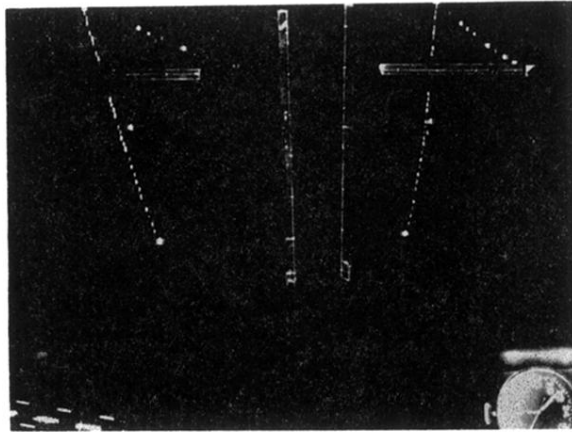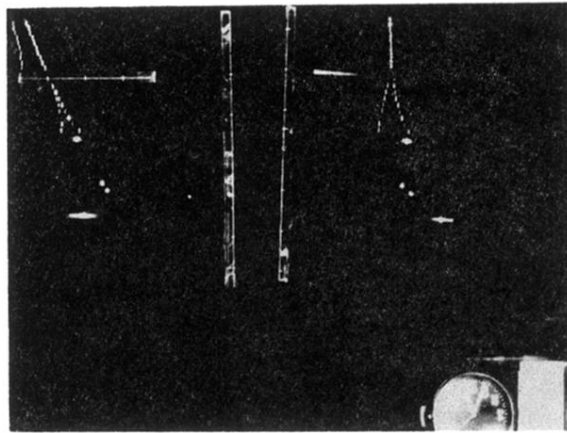FIG. 5. An example of a Λ^0 event in a spark chamber photograph.

FIG. 6. Spark-chamber photograph of an electron pair from a photon converted in the plates of the thin foil spark chamber.